Thermo-mechanical analysis for exhaust manifold using elasto-viscoplastic chaboche model

Hojjat Ashouri

Department of Mechanical Engineering, Varamin-Pishva Branch, Islamic Azad University, Varamin, Iran

ARTICLE INFO	ABSTRACT
	The confluence area cracks are one of the most important durability problems in internal combustion engines. The aim of this article is to present thermo-mechanical analysis for exhaust manifold using elasto-viscoplastic Chaboche model. The Chaboche model was selected for the elasto-viscoplastic model including a kinematic hardening plastic law coupled with the Norton creep equation. The modeling, meshing and analyzing were performed on a finite element model of the exhaust manifold in ABAQUS software. In order to increase the accuracy of finite element analysis (FEA) results, temperature-dependence of material parameters was considered. The results of mechanical-thermal analysis showed that the maximum temperature and stress are visible in the confluence area. Obtained FEA results proved the manifold gasket leak is another critical region that has to sustain the expanding and contracting of the heated exhaust manifold metal. The results of the modal analysis proved that the maximum strain energy density and total strain energy exist in the confluence area. The results of the thermo-mechanical analysis are compared with the real sample of the damaged exhaust manifold to evaluate the properly results, and it has been shown that serious identified zones correspond to the failure areas of the real sample.

1. Introduction

Exhaust manifold collects combustion gases from the engine and directs them to the exhaust system. It plays a prominent role in engine performance. In particular, the amount of pollutants and fuel consumption depends on the exhaust manifold design. As a result, designing a high-reliability exhaust manifold is essential to meeting these requirements. Due to the conflicts of the weight loss and significant thermal loads of the engine, thermal fatigue failure of engine components occurs easily due to excessive engine temperature gradients and heat stress. The exhaust manifold withstands intense thermal cycles between ambient temperature and approximately 850°C. Due to mechanical constraints, these cycles create complex stress and strain that may

cause thermo-mechanical fatigue (TMF). The exhaust manifold must withstand cyclic thermo-mechanical loads throughout the life cycle [1,2]. Exhaust manifolds are damaged by oxidation, fatigue and creep during engine operation. Oxidation occurs due to high engine temperatures with exposure to exhaust gases and exposure to outside air. Thermal loading with limited freedom of expansion causes low cycle fatigue and vibrations cause high cycle fatigue. The effect of creep is twofold and it works through fatigue. By creating cavities, it reduces fatigue life and increases by relaxing stresses [3,4]. Permanent deformation and inelastic response of loaded materials with constant stress and high temperature is called creep, which is time dependent. Creep stress analysis has a long

history in engineering due to design requirements for high temperatures. Constant high stress leads to creep of these structural elements. Creep modeling in multi-axial stresses is the main step in properly predicting long-term structural behavior [5,6]. The exhaust manifold temperatures can rise rapidly from ambient temperature to around 900°C, so exhaust manifold requires excellent heat resistance, great oxidation resistance, and prominent creep performance [3]. Stainless steels are widely used as the material of exhaust manifold due to their corrosion resistance, high heat resistance and recyclable. The 409 Ferritic Stainless Steels (FSS) are often used as exhaust component due to its good resistance to chloride-induced stress corrosion cracking, high temperature resistance, good resistance to oxidation and corrosion and sufficient thermal fatigue resistance [7,8].

Numerous researches have been done on stress analysis fatigue life for exhaust manifolds. Assessment of thermal barrier coating in low cycle fatigue life for exhaust manifold was performed by Ashouri. The results of low cycle fatigue showed that the number of failure cycles for coated exhaust manifolds is almost twice the results obtained for uncoated exhaust manifolds [9]. Salehnejad et al. Developed a finite element method and critical failure resistance to analyze the failure of an exhaust manifold. Their research ruled out the possibility of failure in all spots [10]. Ashouri simulated the thermal-mechanical fatigue of manifolds. The results of finite element analysis showed that temperature and heat stresses have the highest critical values in the confluence region. This area was subjected to cyclic tensile and compressive stresses and then to low cyclic fatigue [11]. Castro Güiza et al. investigated thermal fatigue fracture of exhaust manifolds. Their analysis showed that some areas of the exhaust manifold entered into yield region. Hence, fatigue cracks are observed in them [12]. Azevedo Cardoso and Claudio Andreatta evaluated the thermal-mechanical fatigue of diesel engine exhaust manifolds. Their research ruled out the possibility of failure in all spots [3]. The effect of fin attachment on reducing the thermal stress of exhaust manifolds was investigated by Partoaa et al. Their studies showed that the combined changes, i.e. the thickness increase and the fins attachments, decrease the thermal stresses by up to 28% and the contribution of the fin attachment in this reduction was much higher compared to the shell thickness increase [13]. Ahmed et al. simulated the thermo-structure stresses of tractor exhaust manifolds. Their finite element analysis proved that the stresses

generated during operation for the 321-Austenitic stainless are in the safe zone. TMF was the main cause of exhaust manifold failure [14]. Some correlations presented by other studies for four-stroke engines were evaluated by Lujan et al. They proposed a new heat transfer model for exhaust . Slight differences were observed in the scavenge process related parameters between this model and other models [15]. Low and high cycle fatigue life of the exhaust manifolds were investigated by Lee et al. A good correlation was shown between the experimental and simulated results [16]. The effect of perimeter fins on low cycle fatigue life for exhaust manifold was studied by Ashouri. The results of his analysis showed that the number of failure cycles for the modified exhaust manifold is approximately 55% higher than the results obtained for the original exhaust manifolds [17]. Investigation of elastic, plastic and viscous behavior of the exhaust manifolds was investigated by Santacreu et al. Their research revealed the viscous strain is significant and its amount is not negligible [18]. Vyas et al. studied the CFD-FEA analysis of diesel engine 6-cylinder exhaust manifolds. A good agreement was shown between the experimental and simulated results of the temperature distribution [19]. Transient thermal analysis of exhaust manifolds was performed by Elsharkawy et al. A good agreement was observed between the experimental and simulated temperature results [20]. Ashouri simulated the effect of temperature on modal analysis for the exhaust manifold. The results of finite element analysis showed that gas pressure is effective in modal analysis and should be considered in exhaust manifold analysis [21].

According to research, the fatigue life for exhaust system due to high temperature engine gases is generally divided into three separate failure mechanisms: oxidation damage, creeping damage and mechanical (plasticity) damage [3,4]. In previous papers, some studies have been conducted on oxidation and plasticity, while creep has been significantly less studied. Due to the fact that the exhaust manifold is exposed to high temperatures, the creep considerations become critical [5,22]. The 409 FSS has creep behavior and should be taken into account [7,8]. Therefore, the purpose of this paper is to simulate the thermo-mechanical behavior of the exhaust manifold based on the elasto-viscoplastic Chaboche model. It has been proven that the Chaboche model is generally more computationally efficient than the Sehitoglu model [23]. The use of time-dependent material properties increases the accuracy of FEA results

[13,17]. Therefore, the effect of time-dependent properties for exhaust manifold is also considered in this study.

2. Methodology

2.1. The material behavioral model

The material used for the exhaust manifold is the 409 FSS. Temperature dependent stress-strain curves have been taken from experimental results of [24]. The elasto-viscoplastic behavior of a metal subjected to cyclic loading at high temperatures is well illustrated using a non linear kinematic and isotropic hardening coupled with a Norton creep model such as the unified model proposed by J.L. Caboche [26]. This model predicts the cyclic stress-strain behavior of the material with appropriate accuracy [26,27,28,29]. The constructor models used are all based on the theory of infinitesimal strain theory. Strain partitioning in thermal(th), elastic(el) and viscoplastic (vp) parts gives [26,30]:

$$\underline{\varepsilon} = \underline{\varepsilon}_{th} + \underline{\varepsilon}_{el} + \underline{\varepsilon}_{vp} \tag{1}$$

Where the thermo-elastic part of the strain is defined by the expression:

$$\underline{\varepsilon}_{el} = \frac{(1+\nu)}{E}\underline{\sigma} - \frac{\nu}{E}.Tr(\underline{\sigma})\underline{I} \tag{2}$$

$$\underline{\varepsilon}_{th} = \alpha \Delta T.\underline{I} \tag{3}$$

Where E is the young's modulus, ν is the Poisson's ratio, σ and I are the stress tensor and the second-rank unit tensor, Tr expresses the trace of a second rank tensor, α is the coefficient of thermal expansion and ΔT is the temperature difference. The yield criterion includes both isotropic and kinematic hardening and it is given by the equation [26, 27]:

$$J_2(\underline{\sigma}-\underline{X})-R \geq 0 \tag{4}$$

With

$$J_2(\underline{\sigma}-\underline{X}) = \left[\frac{3}{2}\left(\underline{\sigma}'-\underline{X}'\right)\cdot\left(\underline{\sigma}'-\underline{X}'\right)\right]^{0.5} \tag{5}$$

Where X is the back stress and R is the isotropic hardening. The superscript (') indicates deviator of the tensor. Therefore viscoplastic strain rate is as follows [26, 27]:

$$\underline{\varepsilon}_{vp} = \frac{3}{2}\dot{p}\frac{\underline{\sigma}'-\underline{X}'}{J_2(\underline{\sigma}-\underline{X})} \tag{6}$$

Where

$$\dot{p} = \left[\frac{J_2(\underline{\sigma}-\underline{X})-R}{K}\right]^n \tag{7}$$

Where K and n are temperature dependent parameters.

The non-linear back stress X is finally given by [26, 28]:

$$\underline{\dot{X}} = \frac{2}{3}C\underline{\varepsilon}_{vp}-DXp \tag{8}$$

Where C and D are material constants.

Creep is expressed as a time-dependent plastic behavior at high temperatures and constant stresses. The temperature and stress must be sufficiently high to obtain the creep deformation. Typically, 0.5Tmelt is defined as a critical temperature for the onset of Norton's creep (Equation 9), expresses the relationship between steady state, secondary creep strain velocity and applied stress [26,30]. This model is well-established and validated to apply for most pure metals and many alloys[30]:

$$\dot{\varepsilon}_v = A_0 exp(-\frac{Q}{RT})\sigma^m \tag{9}$$

Where A_0 is the creep constant, Q is the activation energy for creep, R is the universal gas constant, T is the absolute temperature and m is model parameter.

Heat transfer by conduction per unit area per unit time, q̇, in steady situation is defined by the equation [31]:

$$\dot{q} = -k\nabla T \tag{10}$$

Where k is the thermal conductivity and ∇T is temperature difference. In addition gas convection acting on the inside of the exhaust manifold, also external convection and radiation are effective in temperature distribution. Free and forced convection contribute to the convective heat flux in the exhaust system. In this study, the contribution of free convection to the total external heat transfer was ignored and the convection component was expressed only by a forced convection heat transfer correlation [1,16, 32].Heat flux is given by the following expression [32]:

$$\dot{q} = h_{air}(T_{wout}-T_{air}) \tag{11}$$

$$\dot{q} = h_{gas}(T_{wint}-T_{gas}) \tag{12}$$

Where h_{air} is the air heat convection coefficient, T_{out} is the manifold outer surface temperature, T_{air} is the ambient temperature, $h_{gas}$is the gas heat convection coefficient, T_{win} is the manifold outer surface temperature and T_{gas} is the exhaust gas temperature. Heat loss due to thermal radiation between the manifold surface and environment is

predicted by the standard Stefan–Boltzmann equation [31]:

$$\dot{q}=\varepsilon\sigma(T_{win}^4-T_{air}^4) \qquad (13)$$

Where ε is the emissivity and σ is the standard Stefan–Boltzmann constant.

2.2. The finite element model and material properties

TMF analysis of each component requires the cyclic stress-strain distribution. Hot engine components have complex geometry and loading, and it is impossible to use analytical methods to detect the stress-strain distribution in them. Many researchers have used finite element method to obtain stress-strain distribution in of geometrically complex components [11, 17]. The exhaust manifolds analyzed in this article are depicted in Fig. 1.
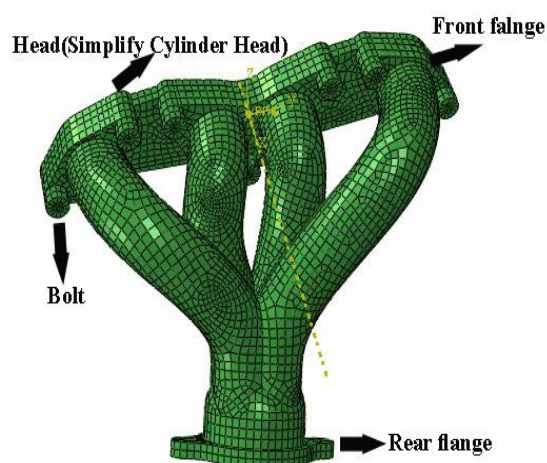

Figure 1: The meshed exhaust manifold[31]

Exhaust manifolds consist of a four tube exhaust manifolds with three flanges, bolted with seven bolts to a small section of the engine head [11]. The manifold is cast from 409 FSS with a Young's modulus of 200GPa, a Poisson's ratio of 0.3, and a coefficient of thermal expansion of 11×10^{-6} per °C [24, 25]. The head is made from aluminum, with a Young's modulus of 69 GPa, a Poisson's ratio of 0.33, and a coefficient of thermal expansion of 22.9×10^{-6} per °C. The bolts are made from steel, with a Young's modulus of 207 GPa, a Poisson's ratio of 0.3, and a coefficient of thermal expansion of 13.8×10^{-6} per °C. The model (manifolds, heads, and bolts) are modeled with three-dimensional continuum elements. The assembly consists of 7450 first-order brick elements with incompatible deformation [11].

2.3. Analysis procedure

Thermo-mechanical analysis for exhaust manifolds is as follows:

1. Apply the prescribed bolt forces to tighten the exhaust manifold to the cylinder head

2. Subject the exhaust manifolds to the transient thermal analysis

3. Return the model to the ambient temperature

4. Gas pressure and temperature distribution data are used to simulate thermo-mechanical stress analysis

5. Thermal modal analysis

3. Results and Discussion

3.1. Apply prescribed bolt loads

The clamping forces introduced by bolts fastening and the material expansion–contraction due to temperature variation during the engine operation are the main loads for thermo-mechanical analysis of exhaust manifolds [3, 11]. Stress and strain have been taken after three cycles applied on the exhaust manifold for thermo-mechanical analysis evaluation, as depicted in Fig. 2 [3]. A typical manifold bolt behavior is shown in Fig. 3. The loads carried by the bolts increase significantly during the heat-up step. The loads do not return precisely to the original bolt load specification upon cool down because of the residual stresses, plastic deformation, and frictional dissipation that developed in the manifolds [11]. In the first step of the analysis, each of the seven bolts is fastened to a uniform bolt force of 20 kN. In Fig. 4 is illustrated vectors of the maximum principal stress. As the Figure indicates the maximum principal stress is tensile. This corresponds to the results by [3, 11, 32].
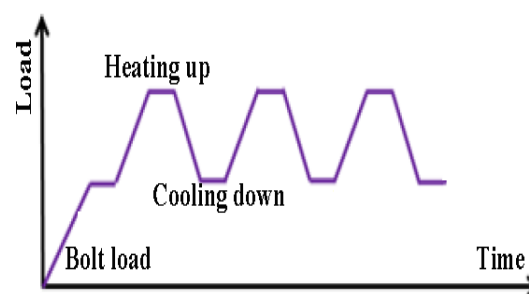

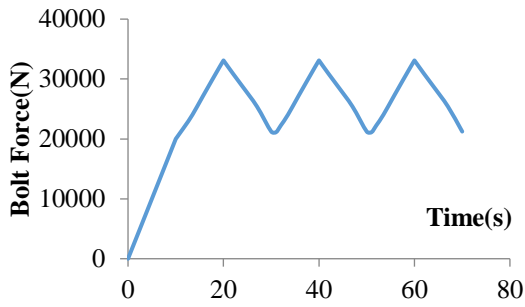**Figure 2:** Schematic cyclic loading for exhaust system analysis

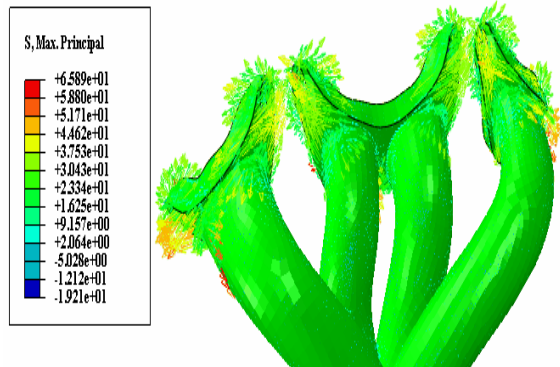**Figure 3:** Typical force variation for manifold load

Figure 4: The maximum principal stress vectors in the exhaust manifold

3.2. Thermal Analysis

The main fluctuation in of heat load is due to the engine start-stop cycles and involves large temperature variations. The heat flux changes due to the fluctuations in of load in different cases. As a result, additional minor heat cycles are created. The ability to accurately predict the exhaust manifold temperature is crucial for a robust/durable exhaust manifold design. Therefore, the first step of a thermo- mechanical analysis is a transient thermal analysis with the aim of predicting the temperature distribution for the exhaust manifold. Thermal loading has a significant effect on the TMF life. The temperature distribution not only identifies important locations but also determines the limitation of the number of cycles to failure [1, 9, 17].

The manifolds are cast from 409 FSS with a thermal conductivity of 25.7 W/m°C, a density of 7700 kg/m³, and a specific heat of 466 J/kg°C [25]. The exhaust manifolds start the analysis with an initial temperature of 20°C. The combustion gases generate a heat flux applied to the surfaces of the inner tube. In this paper, this result is created using a surface-based film condition, with a constant temperature of 816°C and a film condition of $500*10^{-6}$ W/mm²°C. A temperature boundary condition of 355°C is defined at the flange surfaces attached to the cylinder head, and

a temperature boundary condition of 122°C is defined at the flange surfaces attached to the exhaust [11]. Three exhaust gas temperature cycles are applied in the transient thermal analysis for the entire simulation time of 2700s. Every thermal cycle consists of two stages: heating the exhaust manifolds to the maximum operating temperature and cooling it to the minimum operating temperature [1, 2, 16]. From the transient thermal analysis, the temperature distribution can be easily predicted, as shown in Fig. 5. It is maximized in the confluence area. This finding corresponds to the results by Sissaa et al. (2014) and Ashouri (2018, 2019, 2021).
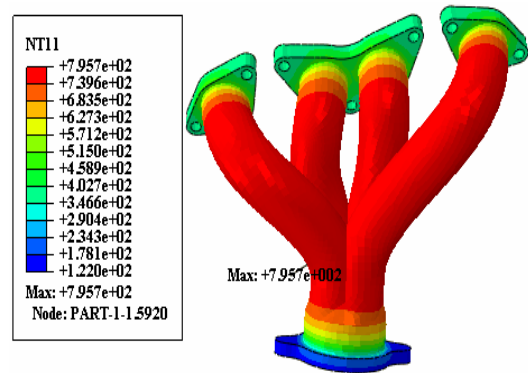

Figure 5: The temperature distribution in the exhaust manifold

The calculated temperature as a function of time at a point in the junction area where four manifold tubes coverage is shown in Fig. 6. As the figure shows from the engine start, the temperature would rise slowly until it was stable and then it was obviously decreasing. The temperature curve trend was close to a straight line from 450~460s, which means that the exhaust manifold temperature reached a steady state. The temperature decreased significantly from 460s to the end of the cycle.
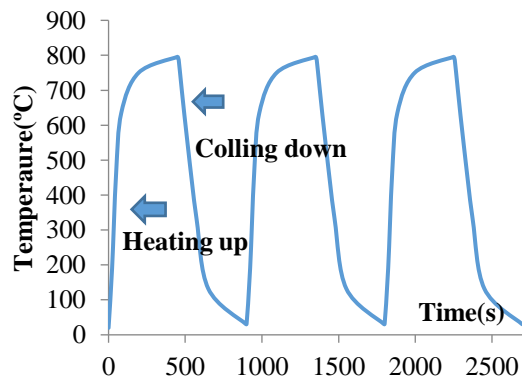

Figure 6: The temperature variations in the hottest spot for three start-stop cycles

3.2. Mechanical analysis

Stresses and strains generated by thermal fields and mechanical loads are calculated by mechanical analysis. [2, 16, 35]. The nonlinearity of the material is considered. The most important boundary condition for stimulating mechanical analysis is the temperature distribution. The complete finite element model shows the working conditions close to the actual conditions. In this assembly it is necessary to specify and to define contacts between all the components. The superposition of the temperature fields is done after the thermal analysis is completed. The temperatures predicted by the previous thermal analysis have been imported in the mechanical analysis as thermal fields [3, 9, 11]. Actual boundary conditions are shown by constraints and contacts between assembly components. It is supposed that the exhaust manifolds are securely fixed to a stiff and bulky engine cylinder head and catalyst, so the rear flange and head surfaces are constrained in the direction normal to the cylinder head and catalyst but are free to move in the two lateral directions to account for thermal expansion. The structural boundary conditions applied to finite element model of exhaust manifold for structural analysis are shown in Fig. 7. Gas pressure of the exhaust manifold is another boundary condition [13, 17].
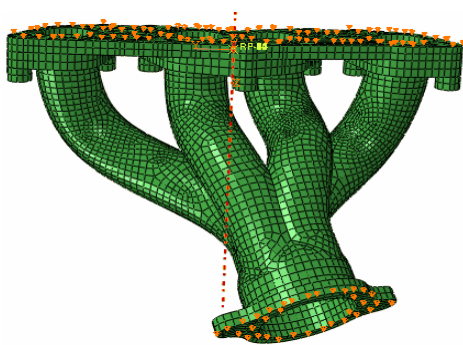

Figure 7: Structural boundary conditions

Fig. 8 depicts the Von-Mises stress distribution at the end of the second step. The maximum value of Von-Mises stress in the exhaust manifolds is predicted 477.5 MPa. Comparing this result to the yield stress of the exhaust manifolds can be a criterion for the crack initiation. This result can lead to crack initiation. The maximum Von-Mises stress occurred in the confluence area, except for the areas around the screws where there was stress concentration. This corresponds to the results by Partoaa (2017) and Ashouri (2019, 2021). As mentioned by Ashouri (2019), the first fatigue cracks can be seen in the hottest point of the

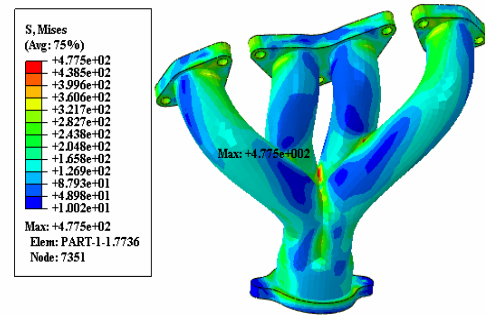exhaust manifolds (Figure 3). This region is also located in the confluence region.

Figure 8: The Von-Mises stress distribution at the end of the third stage of loading

Exhaust manifold deformed under unstable situations. The maximum deformation and its location are generally used to determine whether the product meets the required standards [21, 35]. It can be seen from Fig. 9 that the thermal deformation of front flange and outlet were gradually increasing. The maximum deformation occurs in the rear flange and the value is 1.747mm.
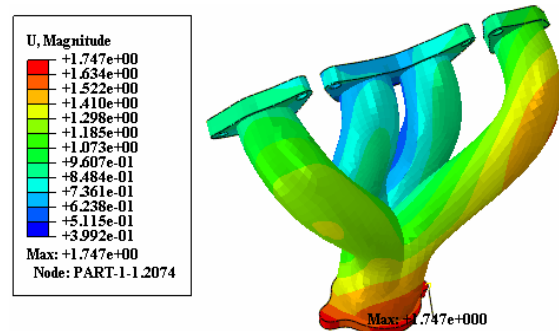

Figure 9: Thermal deformation of exhaust manifold

The lateral displacement of the lower surface of the front flange at the end of the heating step is depicted in Fig. 10. The ends of the two outer manifold flanges have expanded outward relative to one another by only about 0.042 mm due to the frictional sticking. Plastic yielding situations result since thermal expansion of the remainder of the manifold is constrained by this limited lateral flange motion.
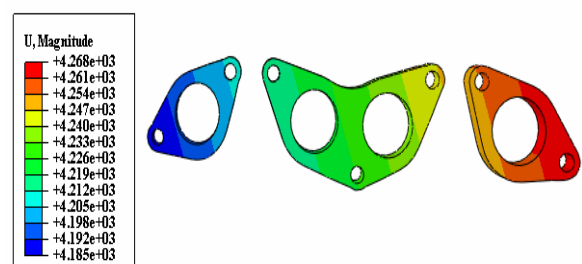

Figure 10: Lateral expansion of manifold footprint

The exhaust hot gases pass through the inner wall of the exhaust manifold, so the component is subject to cyclic thermal loads as the engine heats up and cools down as it is started and stopped. Thermal plastic strain accumulates in the manifold due to cyclic thermal stress, and that eventually adversely affects the lifetime of the manifold as thermal fatigue cracks develop [3, 12, 13, 16]. The mechanical analysis is continued until the strain history shows stabilization. Calculated strains are so high that manifold material exceeds yield limit in several regions of manifold. The field of stresses and pressures makes it possible to identify the most critical region for the integrity of the structure during its fatigue life [2]. The equivalent plastic strain distribution in the exhaust manifold is shown in Fig. 11, which is calculated after using the thermal cycle evaluated by the previously reported thermal analysis. By reviewing the mechanical analysis results, it can be seen that both the stress and plastic strain, which have the dominant effect on the damage evolution are maximum at the junctions (critical areas) where the expansion of the tubes is restricted by flanges and the cylinder head.
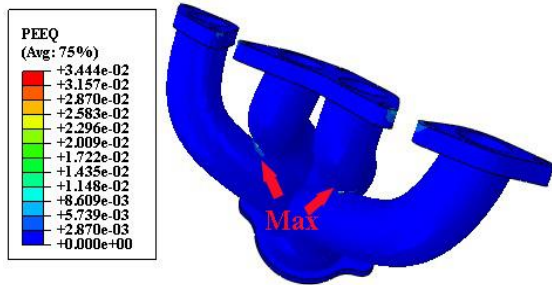

Figure 11: The equivalent plastic strain distribution

The main factor in mechanical-thermal analysis is the temperature distribution of the exhaust manifold, because thermal fatigue crack and gasket leakage can be initiated by thermal deformation caused by temperature fluctuations [1, 2, 35, 36]. Another important parameter to study the gas leakage near the engine side flange during heating and cooling is the opening of the manifold flange gap [1, 34].

Figs. 12 and 13 depict the predicted FEA distance between the engine head and the front flange surface when the engine heats up and cools down, respectively. Fig. 14 shows that because of the expansion of the outer runners under hot situations, the flange bulges out with respect to stiff cylinder head generating some gap in the mid region of the flange. As the engine cools, the outer runners contract and open up the gap near the outer edge of the flange. It should be noted that

the manifold expansion and contraction happens in the plastic regime of stress-strain curve, the gap doesn't come back to zero. The finite element analysis estimated that maximum gap opening near the two outer edges 0.0149mm. This corresponds well with the experimental results as shown in Figure 14.
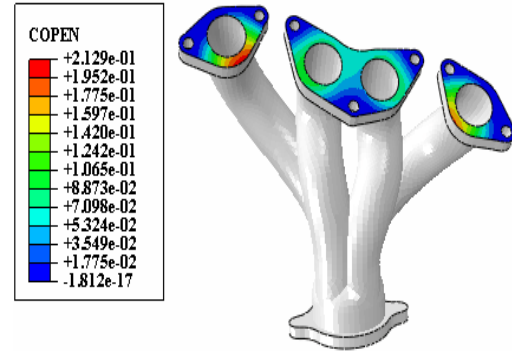

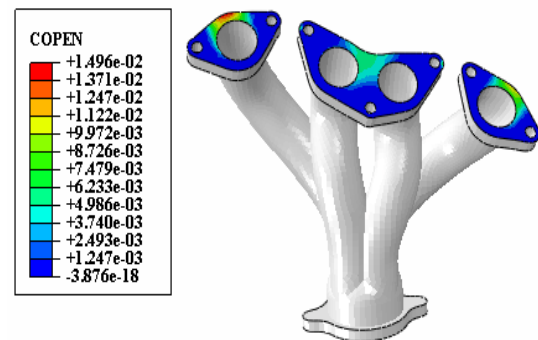**Figure 12:** The manifold gap between the front flange and engine head when the manifold is hot

Figure 13: The manifold gap between the front flange and engine head after the manifold is brought down to lower temperatures.

Figure 14: Evidence of gas leakage on the manifold exhaust

Connection to the engine leads to limited thermal expansion and high temperature gradients. Therefore, the exhaust manifolds withstand cyclic heterogeneous stress, pressure

and temperature. If the temperatures are high and the frequency of thermal changes is low, creep due to stress redistribution can affect fatigue life [22, 37]. The creep strain distribution predicted by Equation (9) is shown in Fig. 15. According to the figure, it is clear that the creep strain is less than the plastic strain and its amount is not negligible. Therefore, creep characteristics should be evaluated in the thermo-mechanical analysis of exhaust manifolds.
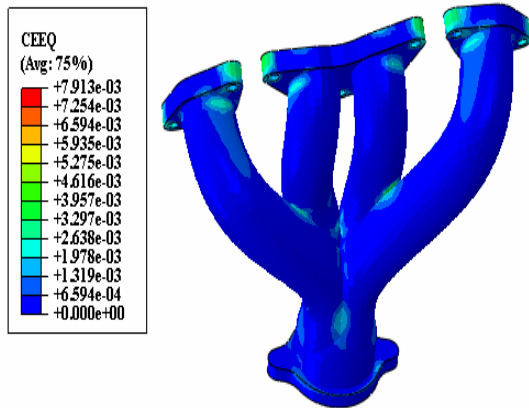

Figure 15: The equivalent creep strain distribution

3.3. Thermal modal analysis

Examining the dynamics of the structure is necessary to understanding and evaluating the performance of each engineering product. The assessment of the dynamic properties of automotive structures is an extremely important issue in the automotive industry. At present, one of the main technologies in structural dynamics analysis is modal analysis. In thermal mode analysis, model analysis with temperature pre-stress and temperature-dependent material properties parameters are investigated [21, 35].

It is worth noting that the distribution of the strain energy density in the exhaust manifold is studied. This energy indicates the most probable point of the failure. The strain energy density is called SENER in ABAQUS software. This parameter is a good criterion for determining failure point in parts [21]. The strain energy density predicts the critical failure points as depicted in Figure 16. The total strain energy is another important variable in determining the failure point. The total strain energy is called ELSE in ABAQUS software. This parameter predicts the failure point of the exhaust manifold in its first natural frequency as depicted in Fig. 17. As it can be seen from Figs. 16 and 17, SENER and ELSE criterions are maximized in the confluence area. Therefore, this area is a serious region and fatigue cracks will initiate in this zone.
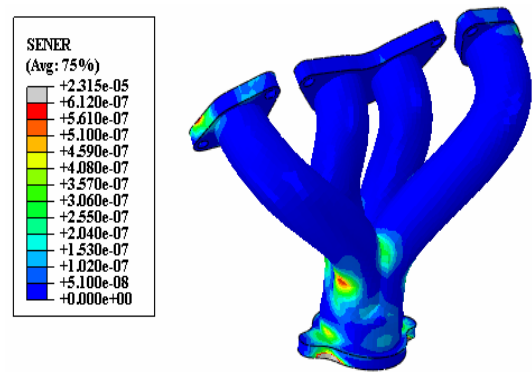

Figure 16: The strain energy density distribution in exhaust manifold
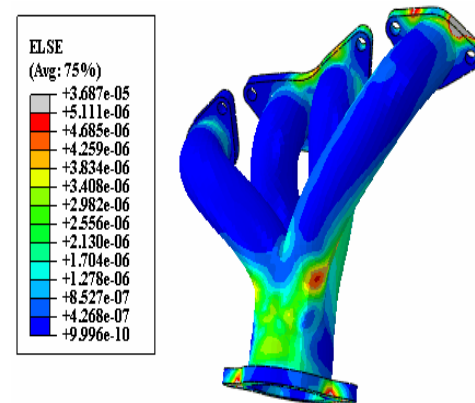

Figure 17: The total strain energy distribution in exhaust manifold in its first natural frequency

The crack experimentally detected is visible in Fig. 18. This crack is created in the same locations predicted by the simulation. Therefore, elasto-viscoplastic Chaboche model is then able to predict the failure point.

Figure 18: The cracked exhaust manifold [38]

4. Conclusion

In this article coupled thermo-mechanical analysis for exhaust manifolds is investigated. A elasto-viscoplastic Chaboche model is utilized for this goal. Finite element analysis allows accurate and reliable prediction of thermo-mechanical and

fatigue results in exhaust manifolds. The results of mechanical-thermal analysis showed that the maximum temperature and stress are visible in the confluence area. Obtained FEA results proved that the manifold gasket leak is another critical region that has to sustain the expanding and contracting of the heated exhaust manifold metal. The creep strain is less than the plastic strain and its value is not negligible. The results of the modal analysis confirmed that the maximum strain energy density and total strain energy are observed in the confluence area. The results of the finite element analysis correspond with the experimental tests, performed in references, and indicate the exhaust manifold failed in this area. In order to prevent exhaust manifolds rupturing it is recommended to change geometry of material in serious components. TBC might also be used which not only reduces temperature and stress, but also increases the fatigue life of exhaust manifolds. Because they reduce thermo-mechanical stresses, fatigue life of the exhaust manifolds increases [9].

References

[1] M. Chen, Y. Wang, W. Wu, J. Xin, Design of the Exhaust Manifold of a Turbo Charged Gasoline Engine Based on a Transient Thermal Mechanical Analysis Approach, SAE Technical Paper 2014-01-2882, (2014).

[2] L. Zhien, X. Wang, Z. Yan, X. Li, Y. Xu, Study on the Unsteady Heat Transfer of Engine Exhaust Manifold Based on the Analysis Method of Serial, SAE Technical Paper 2014-01-1711, (2014).

[3] A-D. Azevedo Cardoso, D. Claudio Andreatta, Thermomechanical Analysis of Diesel Engine Exhaust Manifold, SAE Technical Paper 2016-36-0258, (2016).

[4] C. Öberg, B. Zhu, S. Jonsson, Creep, strain and oxidation damage in the ferritic ductile cast iron SiMo51 at 700°C, Journal of material at high temperature, Vol. 37, No.3, (2020), pp.178-195.

[5] P-O. Santacreu, L. Faivre, A. Acher, Life Prediction Approach for Stainless Steel Exhaust Manifold, SAE Technical Paper 2012-01-0732, (2012).

[6] V. Kobelev, Some basic solutions for nonlinear creep, International Journal of Solids and Structures, Vol. 51, (2018), pp.3372-3381.

[7] W. Xijia, L. Lafleur, Z. Zhong, Thermo-Mechanical Fatigue Testing of Welded Tubes for Exhaust Applications, SAE Technical Paper No. 2018-01-0090, (2018).

[8] R.S. Vidyarthy, D.K. Dwivedi, A comparative study on creep behavior of AISI 409 ferritic stainless steel in as-received and as-welded condition (A-TIG and M-TIG), Journal of Materials Today: Proceedings, Vol. 5, (2018), pp.17097-17106.

[9] H. Ashouri, Evalluation of thermal barrier coating in low cycle fatigue for exhaust manifold, Journal of Simulation & Analysis of Novel Technologies in Mechanical Engineering, Vol. 12, No.4, (2019), pp.41-51.

[10] M.A. Salehnejad, A. Mohammadi, M. Rezaei, Cracking failure analysis of an engine exhaust manifold at high temperatures based on critical fracture toughness and FE simulation approach, Journal of Engineering FractureMechanics,DOI.org/10.1016/j.engfracmech.2019.02.005, (2019). pp. 1-54.

[11] H. Ashouri, Thermo-mechanical fatigue simulation of exhaust manifolds, Journal of Simulation & Analysis of Novel Technologies in Mechanical Engineering, Vol. 11, No.2, (2018), pp.59-66.

[12] G. M. Castro Güiza, W. Hormaza, R. Andres, E. Galvis, and L.M. Méndez Moreno, Bending overload and thermal fatigue fractures in a cast exhaust Manifold, Journal of Engineering Failure Analysis, doi: 10.1016/j.engfailanal.2017.08.016, (2017).

[13] A.A. Partoaa, M. Abdolzadeh, M. Rezaeizadeh M, 2017, Effect of fin attachment on thermal stress reduction of exhaust manifold of an off road diesel engine, DOI: 10.1007/s11771-017-3457-1, (2017), pp.546-559.

[14] F. Ahmad, V. Tomer, A. Kumar, PP. Patil, 2016, FEA Simulation Based Thermo-mechanical Analysis of Tractor Exhaust Manifold, Springer India, CAD/CAM, Robotics and Factories of the Future, Lecture Notes in Mechanical Engineering, DOI 10.1007/978-81-322-2740-3-18, (2016), pp. 173-181.

[15] J.M. Lujan, H. Climent, P. Olmeda P, Heat transfer modeling in exhaust systems of high-performance two-stroke engines, Journal of

Applied Thermal Engineering, Vol. 69, (2014), pp.96-104.

[16] X. Li, W. Wang, X. Zou, Z. Zhang, W. Zhang, S. Zhang, T. Chen, Y. Cao, Y. Chen, Simulation and Test Research for Integrated Exhaust Manifold and Hot End Durability, SAE Technical Paper 2017-01-2432, (2017).

[17] H. Ashouri, Low cycle fatigue life improvement for exhaust manifold using perimeter fins, Journal of engine research, 2021, The Journal of Engine Research, Vol. 61, (2021), pp.23-34.

[18] P-O. Santacreu, L. Faivre, A. Acher, Life Prediction Approach for Stainless Steel Exhaust Manifold, SAE Technical Paper 2012-01-0732, (2012).

[19] S. Vyas, A. Patidar, S. Kandreegula, U. Gupta, Multi-Physics Simulation of 6-Cylinder Diesel Engine Exhaust Manifold for Investigation of Thermo-Mechanical Stresses, SAE Technical Paper 2015-26-0182, (2015).

[20] A. El-Sharkawy, A. Sami, A. Hekal, D. Arora, and M. Khandaker, Transient Modeling of

[21] H. Ashouri, 2021, Evaluation of temperature effect on modal analysis for exhaust manifold, Journal of engine reserch, Vol. 61, (2021), pp.11-21.

[22] C. Öberg, R. Rablbauer, B. Zhu, S. Jonsson, Monotonic and Cyclic Creep of Cast Materials for Exhaust Manifolds, SAE International Journal of Material and Manufacture, Vol. 12, No.2, (2019), pp.149-162.

[23] M. Jianghui, C. Engler-Pinto, S. Xuming, Comparative Assessment of Elastio-Viscoplastic Models for Thermal Stress Analysis of Automotive Powertrain Component, SAE Technical Paper No. 2015-01-0533, (2015).

[24] D. Seruga, M. Nagode, Comparative analysis of optimization methods for linking material parameters of exponential and power models: An application to cyclic stress–strain curves of ferritic stainless steel, Journal of Materials: Design and Applications, Vol. 0, No.0, (2018), pp.1-12.

[25] Z. Wei, D. Konson, D. Clark, L. Luo, S. Lin, F. Yang, 2013, Characterization and Ranking of Materials for Exhaust Systems Under Thermal-

Cycling Condition, SAE Technical Paper No.2013-01-0512, (2013).

[26] J. Lemaitre, and J. Chaboche, Mechanics of Solid Materials, Cambridge University Press, Cambridge, (1990).

[27] J.L. Chaboche, A review of some plasticity and viscoplasticity constitutive theories, International Journal of Plasticity, Vol. 24, (2008), pp.1642–1693.

[28] H. Ashouri, Thermal barrier coating effect on stress and temperature distribution of diesel engines cylinder heads using a twolayer viscoelasticity model with considering viscosity, International Journal of Automotive Engineering, Vol.7, No. 2, (2017), pp.2380-2392.

[29] H. Ashouri, Thermo-mechanical analysis of fatigue cracks of diesel engines cylinder heads using a two-layer two-layer viscoplasticity model with considering viscosity effects, International Journal of Automotive Engineering, Vol. 6, No.2, (2016), pp. 2163-2175.

[30] W. Hosford, Solid Mechanics, Cambridge University Press, Cambridge, (2010).

[31] J.B. Heywood, Internal combustion engine fundamentals, McGraw-Hill press, (1998).

[32] N. Mamiya, T. Masuda, and Y. Yasushi Noda, Thermal Fatigue Life of Exhaust Manifolds, SAE Technical Paper2002-01-0854, (2002).

[33] ABAQUS/CAE(v6.13-1), User᾿ s Manual, (2013).

[34] S. Sissaa, M. Giacopinia, R. Rosia, Low-Cycle Thermal Fatigue and High-Cycle Vibration Fatigue Life Estimation of a Diesel Engine Exhaust Manifold, Journal of Procedia Engineering, Vol.74 ,(2014), pp.105-112.

[35] Z. Yan, L. Zhien, W. Xiaomin, H. Zheng, Y. Xu, Cracking failure analysis and optimization on exhaust manifold of engine with CFD-FEA coupling, SAE Technical Paper 2014-01-1710, (2014).

[36] L. Meda., Y. Yan Shu, M. Romzek, Exhaust System Manifold Development, SAE Technical Paper No. 2012-01-0643, (2012).

[37] X. Wu, T. Quan, C. Sloss, Failure Mechanisms and Damage Model of Ductile Cast Iron under Low-Cycle Fatigue Conditions, SAE Technical Paper No. 2013-01-0391, (2013).

[38] A. Londhe, V. Yadav, Thermo-structural Strength Analysis for Failure Prediction and Concern Resolution of an Exhaust Manifold, CAE, R&D, Mahindra and Mahindra Ltd,Automotive Sector, Nasik, India, (2007).

[39] H. Ashouri, Low cycle fatigue life prediction of an engine exhaust manifold, Automotive Science and Engineering, Vol. 11, No. 2, (2021), pp. 3560-3568.